DETAILED SEISMIC ASSESSMENT AND IMPROVEMENT PROCEDURE FOR VINTAGE FLEXIBLE TIMBER DIAPHRAGMS

Ivan Giongo[1], Aaron Wilson[2], Dmytro Y. Dizhur[3], Hossein Derakhshan[4], Roberto Tomasi[5], Michael C. Griffith[6], Pierre Quenneville[7] and Jason M. Ingham[7]

ABSTRACT

Currently there is little guidance available on an experimentally-validated detailed seismic assessment procedure for vintage flexible timber diaphragms such as are routinely encountered in New Zealand unreinforced masonry buildings. The results from recent testing of full-scale diaphragms are presented and interpreted with particular attention given to the definition of shear stiffness and shear strength values, whilst acknowledging that the recommendations derive from a small data set. References are provided to information previously published elsewhere to justify the theoretical framework adopted, and the procedure is linked to ASCE 41-13 for guidance regarding diaphragm scenarios that have not been studied by the authors. A procedure is provided to account for the effects on diaphragm response of supplementary stiffness due to masonry end walls. The performance of several diaphragms that were improved with either overlays or underlays is reported as potential proof-tested standard solutions. The assessment procedure is demonstrated by providing a mock worked example of a detailed diaphragm assessment.

INTRODUCTION

New Zealand unreinforced masonry (URM) buildings are typically between 80 and 120 years old, with their timber diaphragms therefore of the same age and usually constructed with native timber species. It is known that the nails used to construct these diaphragms are soft when compared to currently manufactured nails, but equally it is noted that the timber has often hardened from a century of drying and that the diaphragm appears to have 'locked up' from a century of use. Whilst it is recognised that vintage timber diaphragms are flexible, anecdotal evidence and observations from the 2010/2011 Canterbury earthquakes suggest that for many URM buildings large diaphragm displacements were not observed.

Recorded seismic response from instrumented buildings having flexible diaphragms has provided support for past analytical studies, such as by Tena Colunga and Abrams (1996), that have shown that design criteria based on rigid diaphragm assumption are not necessarily conservative when applied to buildings with flexible diaphragms, especially when determining the magnitude of seismic input, as demonstrated by Raggett and Rojahn (1991). Hence there is currently a significant lack of clarity regarding a suitable detailed seismic assessment procedure for vintage flexible timber diaphragms.

Information is presented below to explain the source of the recommendations proposed for a revision to the NZSEE 'Red Book' (NZSEE 2006) that pertain to the detailed seismic assessment of vintage flexible timber diaphragms. It is acknowledged that the stiffness values for straight sheathed diaphragms may require future modification if additional in-situ testing is undertaken that indicates that alternative stiffness values are more appropriate.

Brignola *et al.* (2012) have provided detailed information on relevant past testing related to the seismic performance of flexible timber diaphragms, plus the effect that the stiffness of the wall-diaphragm connections has on the global stiffness of the diaphragm. They have also presented details related to existing diaphragm assessment procedures in USA and Italy, and a prior procedure used in New Zealand.

[1] *Post-doctoral research fellow, Trento University, Trento, Italy*

[2] *Structural engineer, Holmes Consulting Group, Auckland, New Zealand*

[3] *Post-doctoral research fellow, University of Auckland, Auckland, New Zealand*

[4] *Post-doctoral research fellow, University of Adelaide, Adelaide, Australia*

[5] *Assistant Professor, University of Trento, Trento, Italy*

[6] *Professor, University of Adelaide, Adelaide, Australia*

[7] *Professor, University of Auckland, Auckland, New Zealand*

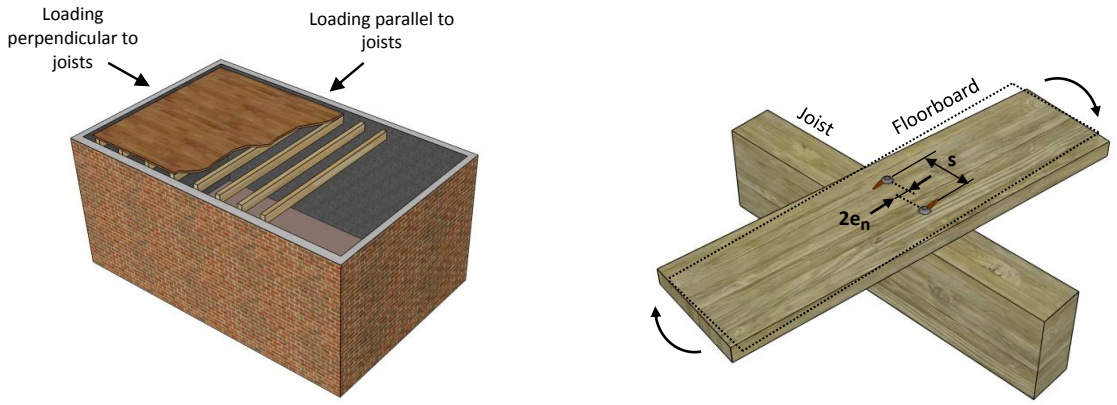

(a) Orthogonal diaphragm response due to joist orientation.

(b) Nail joint rotation due to nail slip and nail spacing.

Figure 1: Schematics showing aspects of diaphragm response.

DISPLACEMENT ACCEPTANCE CRITERIA

In order to develop a detailed seismic assessment procedure for vintage flexible timber diaphragms as found in New Zealand URM buildings it is necessary to first establish a displacement acceptance criteria. Three distinct criterions are promulgated, associated with: (1) limiting the extent of diaphragm distortion; (2) controlling diaphragm displacements to an extent that they minimise detrimental influence on out-of-plane wall deformations; and (3) limiting global building drift ratios.

Limiting diaphragm distortion

Flexible timber diaphragms are known to deform as shear beams (Wilson *et al.* 2013a, 2013b) and to exhibit orthotropic behaviour when loaded in their plane, due to the orientation of the joists (see Figure 1(a)). The diaphragm mid-span displacement can be related to the maximum permissible rotation of nail joint connections (with maximum rotations occurring at the diaphragm boundaries where shear deformations are largest), with nail joint rotation being dictated by the spacing s (in mm units) between the nail couple and the slip in each nail e_n (in mm units) resulting from the applied shear force (see Figure 1(b)). For single straight sheathed diaphragms loaded perpendicular to the orientation of the joists, as per NZSEE (2006) Eq. 11A(2), the relationship is given by:

$$\Delta_{mid} = \frac{Le_n}{2s} \quad (1)$$

where L is the diaphragm span. For straight sheathed diaphragms loaded parallel to the orientation of the joists the corresponding relationship is:

$$\Delta_{mid} = \frac{5}{8} \cdot \frac{Le_n}{2s} \quad (2)$$

As noted in NZSEE (2006) section 11.3.1, the flooring of existing timber diaphragms is usually 25-50 mm thick, with board widths of 100-200 mm. The specific spacing between nails within a nail joint should be measured during a detailed inspection of the diaphragm, but is typically about 75% of the board width and in the order of s = 100 mm.

Limited measured data exists regarding nail slip characteristics for New Zealand vintage flexible timber diaphragms, with Wilson *et al.* (2014b) having reported data for nail connections extracted from several relevant diaphragm samples. A further complication is to establish the tolerable condition of the most extremely loaded nail joints that merits definition of the diaphragm acceptance criteria. Hence it is suggested that 'first yield' (or departure from elastic response) is too restrictive as a criterion for the most severely loaded joints, and instead Wilson *et al.* (2014b) report the nail slip at maximum connection strength as having a mean value of 8.1 mm. Given that there is some variance amongst measured results, a reduction factor of 0.75 is proposed and a nail slip of e_n = 6.0 mm is recommended. Strictly speaking Equations 1 and 2 do not apply once inelastic response occurs within the most severely loaded nail connections of the diaphragm, but recalling that the majority of nail connections within the diaphragm will remain in their elastic state, the relationships are deemed to still be appropriate. Hence it follows that for an assumed s =100 mm Equation 1 would provide Δ_{max} = L/33.33 for loading oriented perpendicular to the joists and Δ_{max} = L/53.33 for loading oriented parallel to the joists. For a URM building having plan dimensions of 8 m × 12 m, a wall thickness at diaphragm height of 230 mm, and with joist spanning the short dimension, the maximum acceptable mid-span diaphragm displacements associated with limiting diaphragm distortion would be 226 mm for loading perpendicular to joist and 216 mm for loading parallel to joist.

Limiting wall instability

Based on experimental results reported by Vaculik (2012) and by Griffith *el al.* (2007), the diaphragm maximum in-plane displacement measured with respect to the diaphragm URM side walls shall not exceed 50% of the thickness of the adjacent URM end walls. For multi-storey buildings consideration must be given to the situation that potentially arises when diaphragms at different storey heights deform out-of-phase. The worst case scenario would develop when the diaphragms on two adjacent levels are 100% out-of-phase (see Figure 2(a)). However, this deformation is considered to be a higher mode with smaller associated displacements and hence is deemed to be too severe as an acceptance criteria, and instead the critical condition is associated with the assumption that the diaphragm at any given storey height is deformed to its maximum mid-span displacement while the diaphragms on adjacent levels are undeformed.

For solid URM walls the wall thickness is likely to be approximately 230 mm for a 2 leaf wall, and so this criterion would result in a maximum diaphragm mid-span displacement of 115 mm (see Figure 2(b)). For solid walls having a greater thickness the acceptable diaphragm mid-span displacement would be proportionally increased.

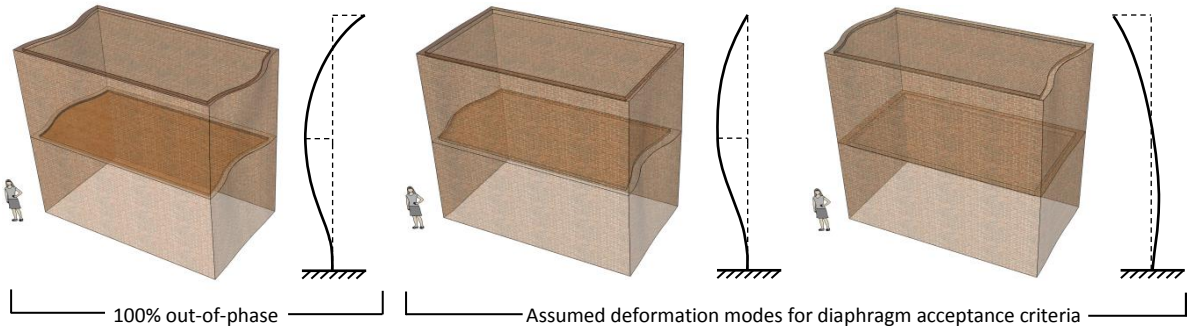

(a) Wall-diaphragm interaction for a multi-storey URM building.

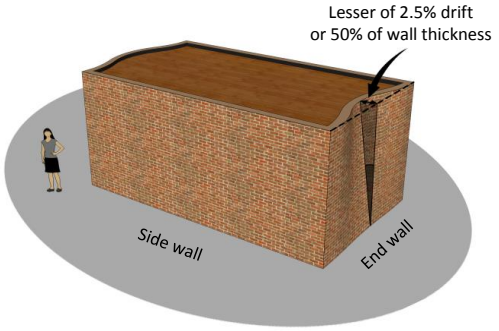

(b) Mid-span diaphragm displacement limit for URM building on a rigid foundation.

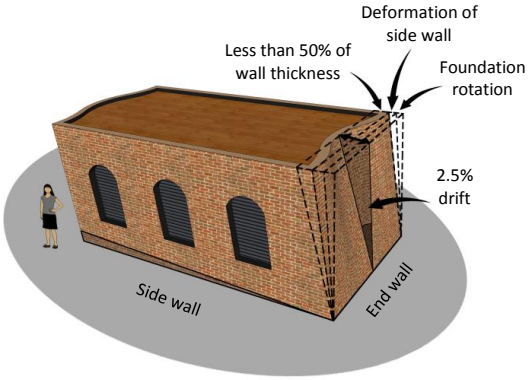

(c) Mid-span diaphragm displacement limit for URM building on a flexible foundation.

Figure 2: Diaphragm displacement acceptance criteria.

For cavity construction with adequate cavity ties installed, the inner masonry wythe is usually the load bearing wythe and this criterion will require the maximum acceptable diaphragm displacement to be limited to 50% of the thickness of the inner wythe. For a cavity wall having a single brick thickness of 110 mm this criterion would result in a maximum permissible mid-span diaphragm displacement of only 55 mm. This criterion may also govern for unusual building configurations.

Limiting building drift

NZS 1170.5:2004 clause 7.5.1 limits inter-storey deflection to 2.5%, including contributions from global building deformation due to foundation rotation (see Figure 2(c)). However, the treatment of building deformations attributable to flexible foundation response is outside the scope of the reported study.

The total mid-span diaphragm displacement relative to the ground (excluding foundation rotation) is composed of deformations due to the in-plane loaded URM side walls and to deformation of the diaphragm with respect to the side walls, with the relative contributions of the two deformation modes being dependent on the characteristics of the diaphragm and wall-diaphragm connections, but also on the characteristics of the URM side walls, such as wall cross-section details and the geometry of wall penetrations.

The information in Figure 3 is reproduced to show that in general the in-plane loaded side walls will deform with small drifts. Note that from Figure 3(b) it can be established that the strength plateau was reached at a roof-height displacement of approximately 10 mm, corresponding to a drift of 0.16% or an inter-storey displacement of 6.2 mm for a wall height of 4,000 mm.

The suggested approach is to assume that in general the URM side walls may be treated as approximately rigid for the purposes of diaphragm assessment, but that for cases where the side walls are particularly slender, heavily penetrated by openings, or there is significant foundation flexibility, more detailed study is required to establish the limiting diaphragm displacement to ensure that a total diaphragm mid-span drift of 2.5% is not exceeded (see Figure 2(c)). Consequently, for a URM building with a storey height of 4,000 mm this criterion will result in an acceptable diaphragm mid-span displacement of 100 mm.

Criterion assumed to govern for the interpretation of physical test data

As the walls of URM buildings typically have inter-storey heights ranging from 3,500 mm to 4,500 mm, a representative height of 4,000 mm has been adopted here and the acceptable mid-span diaphragm displacement is therefore adopted as 100 mm for the treatment presented below. It is noted that this 100 mm mid-span diaphragm displacement will typically correspond to less than 50% of the cross-section thickness of adjacent solid URM walls. However, for an inner load bearing wythe of a cavity wall that has a single brick thickness (usually approximately 110 mm) the limiting mid-span diaphragm displacement will be reduced to 55 mm, emphasising the importance of clearly determining the wall cross-section characteristics. For cavity construction where the inner load bearing wythe is two bricks thick (typically 230 mm), the 2.5% drift criteria for the mid-span diaphragm displacement limit will govern for walls having a height of less than or equal to 4,600 mm.

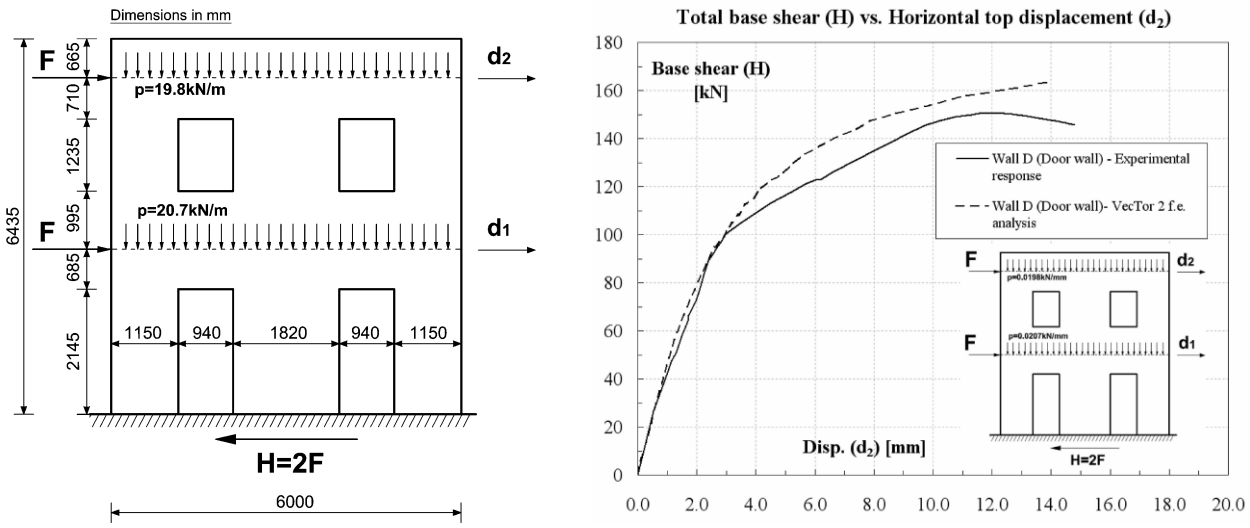

(a) Geometry of a two wythe (250 mm thick) solid URM wall. *(b) Force-displacement response.*

Figure 3: Representative in-plane force-displacement response of a full-scale two-storey wall test [Reproduced from Magenes et al. 1995; Faconni et al. 2013].

DETERMINING EQUIVALENT SHEAR STIFFNESS FOR STRAIGHT SHEATHED DIAPHRAGMS

The force-displacement response of straight sheathed diaphragms is known to be nonlinear, and has been shown to be adequately modelled by second-order curves such as suggested by ABK (1982). Shown in Figure 4(a) is the result of a cyclic test performed by Giongo *et al.* (2013) on a vintage straight sheathed timber floor as typically encountered in New Zealand unreinforced masonry buildings. It can be seen that the as-built vintage straight sheathed flexible timber diaphragm deformed to lateral displacements exceeding the 100 mm acceptance criteria without exhibiting a strength plateau, and hence the diaphragm response can be approximated as an equivalent elastic system over the displacement range of interest. As shown in Figure 4(b), care needs to be exercised when defining the secant stiffness for the diaphragm so that a realistic determination can be made regarding whether the diaphragm has displaced to less than or greater than the acceptable displacement when subjected to ultimate limit state loads.

The most widely respected recommendations for diaphragm stiffness are the data published in ASCE 41-13, which specifies a shear stiffness for straight sheathed diaphragms of 350 kN/m. Such data derive from the studies of ABK (1982) on full-scale (6.1 m × 18.3 m) timber diaphragms. The specimens consisted of 51 mm × 305 mm (2" × 12") Douglas fir joists positioned at 610 mm spacing and having a wood framing system constructed with 102 mm × 305 mm (4" × 12") elements. The flooring was comprised of 25 mm × 152 mm (1" × 6") Douglas fir lumber sheathing, fixed to the joists using two 8d wire nails at each floorboard-to-joist intersection. Three nails were position at the end of each board. 51 mm × 102 mm (2" × 4") Douglas fir blocking elements were also present. However, three concerns with direct adoption of this data are that: (1) it is not clear that the data has specific relevance to vintage diaphragms having the characteristics commonly encountered in New Zealand URM buildings, including wall-diaphragm boundary effects; (2) it is not clear what secant stiffness was used to develop these stiffness values but it is assumed that the data relates to bi-linearisation of the force-displacement envelope with adoption of the initial stiffness, therefore potentially having a substantially greater magnitude than the secant stiffness to a displacement of 100 mm, as indicated in Figure 4(b); (3) no guidance is provided on how to account for the orthotropic nature of the diaphragm and the influence of any possible diaphragm degradation due to insect infestation or moisture damage as is likely encountered in vintage timber diaphragms.

DIAPHRAGMS AS SHEAR BEAMS

Wilson *et al.* (2013a) have confirmed that the deformation

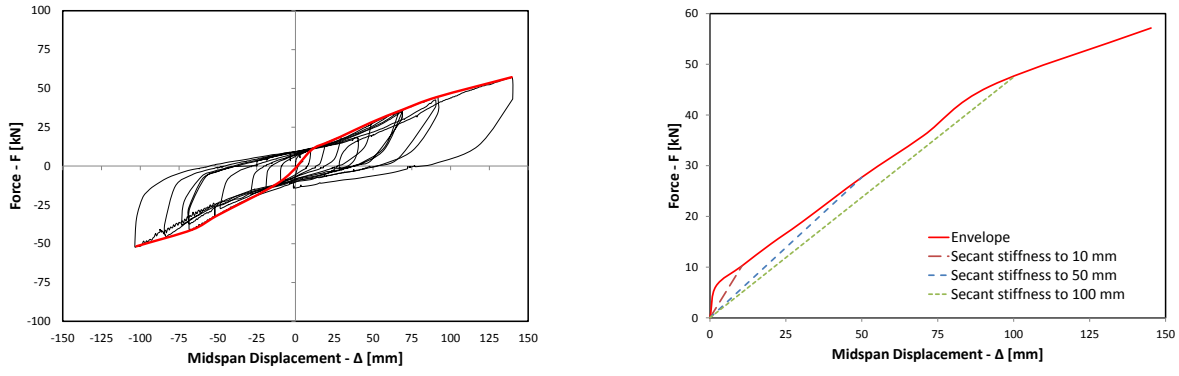

(a) Test data and backbone curve. *(b) Secant stiffness for different acceptance criteria.*

Figure 4: Representative force-displacement characteristics of an as-built straight sheathed vintage flexible timber diaphragm [Giongo et al. 2013].

(a) Evidence of mass-loss due to insect infestation.

(b) Evidence of decay due to moisture.

Figure 5: Deteriorated condition of vintage Whanganui timber diaphragm tested in-situ.

mechanics of flexible timber diaphragms most correctly match that of a shear beam (as has previously been assumed in most assessment procedures). A feature of a shear beam is that both the shear stiffness and the shear strength are proportional to the section depth B. During diaphragm in-plane deformation due to earthquake shaking the deformed profile of the diaphragm is assumed to be approximately parabolic and hence the acceleration profile along the diaphragm is also assumed to be parabolic. For in-plane horizontal diaphragm accelerations due to tributary weight from the two masonry boundary end walls, the diaphragm self-weight, and any imposed live load on the diaphragm, the total lateral force on the diaphragm is defined by $C(T_d)W_{trib}$ where $C(T_d)$ is the horizontal design action coefficient for the diaphragm. $C(T_d)$ is dependent on diaphragm period, which in turn is dependent on diaphragm shear stiffness. Consequently, reliable assessment of vintage flexible timber diaphragms requires accurate estimation of the diaphragm shear stiffness.

For a diaphragm of length L and depth B and assumed to have a rectangular cross-section, the diaphragm mid-span displacement when loaded with a parabolic load having a total value of $C(T_d)W_{trib}$ is defined by Wilson *et al.* (2013b) as:

$$\Delta_d = \frac{3}{16}\frac{C(T_d)W_{trib}L}{BG_d} \qquad (3)$$

where G_d is the diaphragm equivalent shear stiffness. Note that for diaphragms that are bounded on one or both sides by comparatively flexible timber framed partition walls (when compared to the in-plane stiffness of URM solid or cavity walls) there is no experimental test data currently available regarding likely response, and such a scenario will require a specific study. Hence when considering experimental data for sections of diaphragm displaced to 100 mm, the above equation can be re-expressed to establish the experimentally measured secant shear stiffness at 100 mm as:

$$G_d = \frac{3}{160.1}\frac{FL}{B} \qquad (4)$$

where F is the total in-plane force applied to the diaphragm when displaced to 100 mm. As noted in Figure 4(b), the interpretation of physical test data for a mid-span displacement of 100 mm (the governing displacement limit when bounded by solid URM walls) will lead to a slightly conservative estimate of diaphragm equivalent shear stiffness for situations where the diaphragm is bounded by single brick wythe cavity URM walls and the limiting diaphragm displacement is 55 mm.

INTERPRETING TEST DATA TO OBTAIN EQUIVALENT SHEAR STIFFNESS VALUES

It is recognised that it is not possible to make strong recommendations on likely equivalent shear stiffness values when only a small set of field diaphragm test data exists, but Giongo *et al.* (2013) have published the results from in-situ testing of two sections (9.6 m × 5.6 m and 9.6 m × 4.7 m) of a vintage straight sheathed timber diaphragm that were both loaded perpendicular to the orientation of the joists, with the joists oriented parallel to the 9.6 m dimension. The building within which the diaphragm sections were housed was located in Whanganui (lower North Island of New Zealand) and was constructed in 1913, making the diaphragms 99 years old at the time of testing. Both diaphragm test sections were in poor condition, as shown in Figure 5. In order to adequately load the diaphragms it was necessary to remediate the wall-diaphragm anchorages loaded in shear using 16 mm epoxy-grouted anchorages at spacings no greater than 2.0 m. This test data is significant because the diaphragm was constructed of native timber matai floorboards (130 mm × 22 mm) overlying native rimu timber joists (50 mm × 300 mm) with an average spacing of 450 mm. Two wire nails (≈ 2.93 mm × 40 mm) were present at each floorboard-to-joist intersection, with an average spacing of 100 mm. In the region where the joists were overlapped (see Figure 6) there were two wire nails that were considered to provide negligible connection between the joists.

As indicated in Figure 6, the test set-up was self-reacting by enabling loads to be applied back to the building corners and the loading mechanism was designed to approximately replicate the parabolic load distribution anticipated during earthquake excitation. The loading system utilised two opposing cable systems to allowed reversed cyclic loading to be undertaken, with the cables of the opposing loading system being slack for each half cycle of loading. Low friction bearing pads were positioned between the joists and the underlying mid-span supporting timber beam such that potential sources of friction were alleviated.

For the two lateral load tests on the diaphragm that is depicted in Figure 5 and Figure 6, the secant stiffness values at 100 mm of mid-span displacement are reported in Table 1. From Table 1 the effect of joist lap conditions on diaphragm shear stiffness

Table 1: Secant stiffness values for insitu testing of vintage diaphragms loaded perpendicular to joists

Description	L (m)	B (m)	F (kN)	Δ (m)	G_d (kN/m)
Diaphragm A was in poor condition. Some flooring was discontinuous above the location where the joists were lapped (see Figure 6)	9.6	5.6	48.4	0.100	156
Diaphragm B was in poor condition. Most flooring was discontinuous above the location where the joists were lapped (see Figure 6)	9.6	4.7	35.8	0.100	137

Table 2: Secant stiffness values for laboratory testing of new diaphragms loaded perpendicular and parallel to joists

Description	L (m)	B (m)	F (kN)	Δ (m)	G_d (kN/m)
Diaphragm 1a-PERP was tested perpendicular to joists	5.5	10.4	74	0.100	73
Diaphragm 1a-PARA was tested parallel to joists	10.4	5.5	30	0.100	106

is evident. Both diaphragms reported in Table 1 had discontinuous joists, but during testing of Diaphragm B the effect of discontinuous joists was more pronounced due to the greater number of floor boards that were not continuous at the location of joist lap. Wilson (2012) used Finite Element modelling to numerically investigate the effect of joist continuity on diaphragm shear stiffness and found that diaphragms in poor condition and having continuous or lapped joists are 27.5% stiffer than diaphragms with discontinuous joists. This result is confirmed to some extent by the 13% increase in shear stiffness for Diaphragm A where the effect of discontinuous joists was less pronounced due to the greater number of floor boards that were continuous at the location of the joist lap.

Wilson *et al.* (2014a) have published the results from testing of newly constructed flexible timber diaphragms, tested both perpendicular and parallel to the orientation of joists. The equivalent shear stiffness data is presented in Table 2, where it is evident that the shear stiffness of newly constructed timber diaphragms was notably less than the values reported in Table 1 for in-situ testing of vintage flexible diaphragms. This outcome is principally explained by recognising the increased timber density of aged and therefore seasoned timber, which may result in timber densities being elevated by 50%, and the associated influence of timber density on the performance of nailed connections.

From Table 2 it can be established that the ratio of stiffnesses for testing parallel and perpendicular to the joist orientation is approximately 1.45/1.00. This finding is consistent but a little higher than the ratio of 1.30/1.00 obtained by Wilson (2012) using Finite Element modelling. From consideration of these two results, it is assumed that a ratio of 1.33/1.00 suitably

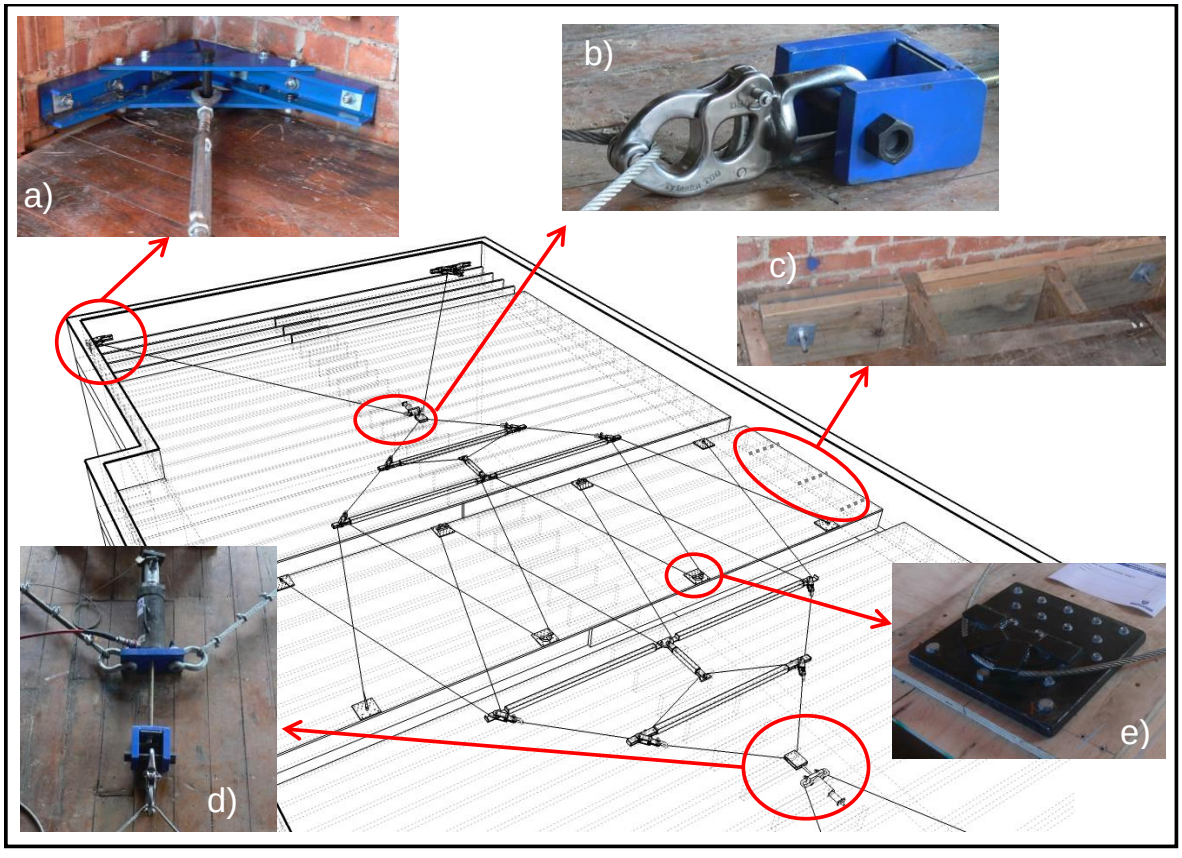

Figure 6: Test set-up for Whanganui diaphragm test; a) wall connection bracket; b) snap shackle for instantaneous load-release; c) new shear anchors; d) hydraulic actuator; e) central loading plate.

Table 3: Shear stiffness values† for straight sheathed vintage flexible timber floor diaphragms

Direction of loading	Joist continuity	Condition rating	Shear stiffness†, G_d (kN/m)
Parallel to joists	Continuous or discontinuous joists	Good	350
		Fair	285
		Poor	225
Perpendicular to joists††	Continuous joist, or discontinuous joist with reliable mechanical anchorage	Good	265
		Fair	215
		Poor	170
	Discontinuous joist without reliable mechanical anchorage	Good	210
		Fair	170
		Poor	135

† Values may be amplified by 20% when the diaphragm has been renailed using modern nails and nail gun
†† Values should be interpolated when there is mixed continuity of joists or to account for continuous sheathing at joist lap

forecasts the stiffness ratio for loading parallel/perpendicular to joist orientation.

The effect of diaphragm condition on diaphragm stiffness was studied by Wilson (2012) using Finite Element modelling to undertake parametric analysis. Kent *et al.* (2005) and Sawata *et al.* (2008) have undertaken physical testing to show that the effects of moisture saturation and insect infestation can substantially influence the stiffness of timber connections, with the extent of the influence extending to reductions of 50% for timber in poor condition. Wilson's numerical model suggested that stiffness values for diaphragms in good condition should be elevated by approximately 50% with respect to that of diaphragms in poor condition. This finding can be used to determine that from Table 1 the forecast shear stiffness of diaphragms tested parallel to joist and being in good condition should have a shear stiffness of approximately 137 × 1.275 × 1.33 × 1.5 = 348 kN/m (experimental stiffness × coeff. for continuous joists × coeff. for loading parallel to the joists × coeff. for diaphragms in good condition). Recalling that ASCE 41-13 recommends a stiffness of 350 kN/m for straight sheathed diaphragms, this value seems plausible and is used to develop the distribution of shear stiffness values shown in Table 3.

Giongo *et al.* (2013) renailed Diaphragm A (previously reported in Table 1) by using 2.85 mm × 75 mm nails, and measured improved stiffness as shown in Figure 7. This finding is consistent with anecdotal evidence that the re-nailing of vintage flexible timber diaphragms elevates their stiffness. On this basis it is recommended that the stiffness

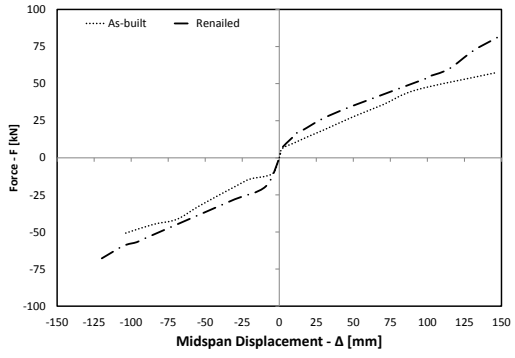

Figure 7: Force-displacement envelope for renailed vintage diaphragm.

values presented in Table 3 be elevated by 20% when the diaphragm is re-nailed at every floorboard-to-joist intersection using modern nails applied by nail gun.

Timber roofs of URM buildings were frequently constructed with both a roof lining and a ceiling lining, and roof linings in New Zealand vintage URM buildings have been observed to sometimes be constructed of either diagonal sheathing or double layers of sheathing. Hence, it is likely that such roof diaphragms are significantly stiffer than are mid-height floor diaphragms. For diaphragms constructed using sheathing types other than straight sheathed (such as may be encountered in roofs) the diaphragm shear stiffness values listed in Table 3 should be multiplied by the values given in Table 4, which are derived from ASCE 41-13. When roof linings and ceiling linings are both assumed to be effective in providing stiffness their contributions should be added.

EFFECT OF DIAPHRAGM PENETRATION

Wilson (2012) undertook Finite Element modelling to investigate the influence of diaphragm penetrations on diaphragm shear stiffness and shear strength and established that for typically sized diaphragm penetrations (usually a rectangular shaped area which accommodates a staircase, corresponding to less than 10% of the diaphragm gross area) linear scaling of the ratio of net to gross diaphragm area was

Table 4: Stiffness multipliers for other forms of flexible timber diaphragms [from ASCE 41-13]

Type of diaphragm sheathing		Multipliers to account for other sheathing types
Single straight sheathing		× 1.0
Double straight sheathing	Chorded	× 7.5
	Unchorded	× 3.5
Single diagonal sheathing	Chorded	× 4.0
	Unchorded	× 2.0
Double layered sheathing (straight or diagonal)	Chorded	× 9.0
	Unchorded	× 4.5

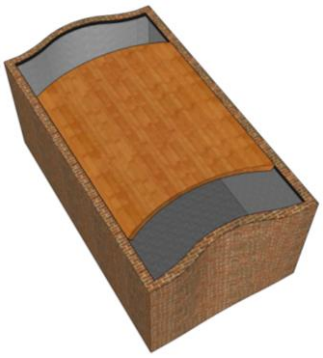

Figure 8: Displacement incompatibility between diaphragm and URM end walls.

appropriate. A special study should be conducted to establish the influence of non-typical sizes of diaphragm penetrations. Therefore a reduced diaphragm shear stiffness (G'_d) to account for the presence of diaphragm penetrations can be calculated as given below.

$$G'_d = \frac{A_{net}}{A_{gross}} G_d \tag{5}$$

ADDED STIFFNESS OF BOUNDARY WALLS

The effective diaphragm shear stiffness must be further modified to account for stiffness of the URM end walls deforming out-of-plane in collaboration with the flexible timber diaphragm. Hence:

$$G'_{d,eff} = \alpha_w G'_d \tag{6}$$

where α_w may be determined using any rational procedure to account for the added stiffness and incompatibility of deformation modes that arise due to collaborative deformation of the URM end walls displacing out-of-plane in flexure and the diaphragm deforming as a shear beam (see Figure 8). Depending on the boundary conditions, the URM end walls may resist out-of-plane deformations by developing two-way bending actions as shown in Figure 8. However, because of the lack of an established procedure to determine the out-of-plane stiffness of two-way spanning walls, simple analytical models were used to provide an estimated value of α_w by instead assuming one-way vertically spanning wall behaviour. Figure 9(a) shows a simplified model of a flexible diaphragm excluding out-of-plane wall stiffness and Figure 9(b) shows a similar model that includes the out-of-plane wall stiffness. In these models m_d refers to the mass of the diaphragm and m_w refers to the mass of the out-of-plane responding URM walls, with the coefficient 2 describing the fact that there are two end walls and the co-efficient ½ describing the tributary mass of these end walls with respect to the diaphragm.

Assuming that the out-of-plane responding walls are cracked at floor levels (see Figure 10) and that they respond in one-way vertically spanning deformation modes as indicated in Figure 2(a), the stiffness contribution from these walls can be calculated by assuming cracked wall rocking action as shown in Figure 10. The contribution to diaphragm shear stiffness from out-of-plane responding walls located in the middle stories of multi-storey buildings can then be calculated as the sum of the stiffness of the cantilever walls in the floors located directly above and below the diaphragm. It is noteworthy that such an approach is conservative as the effect of the applied overburden, such as for the ground storey wall in Figure 10, is ignored.

The timber diaphragm has been modelled as a shear beam spanning between the in-plane loaded side walls, and the distributed mass of the combined diaphragm and two out-of-plane loaded URM boundary end walls has been represented by an equivalent lumped mass corresponding to a generalised single-degree-of-freedom system. Using this modelling approach, the generalised lumped mass for a shear beam is 8/15 of the total mass, as indicated in Figure 9. The degree of freedom is located at the diaphragm mid-span, and k_d represents the diaphragm shear stiffness associated with mid-span displacement and a parabolic load distribution. The natural period for the two systems can be calculated as:

$$T_1 = 2\pi \sqrt{\frac{8}{15 k_d}(m_d + m_w)} \tag{7}$$

and

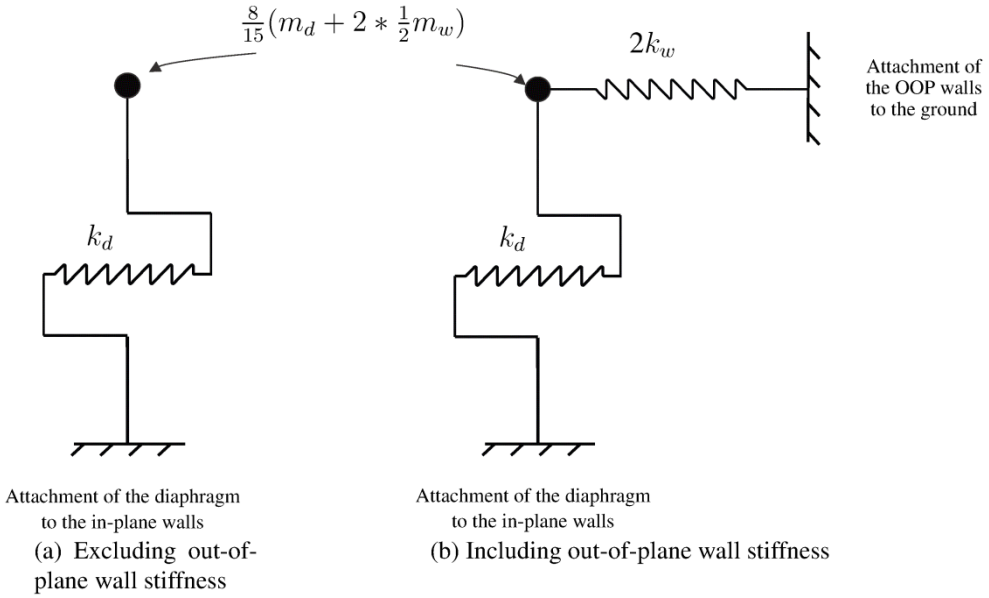

(a) Excluding out-of-plane wall stiffness

(b) Including out-of-plane wall stiffness

Figure 9: Simplified analytical models of diaphragm.

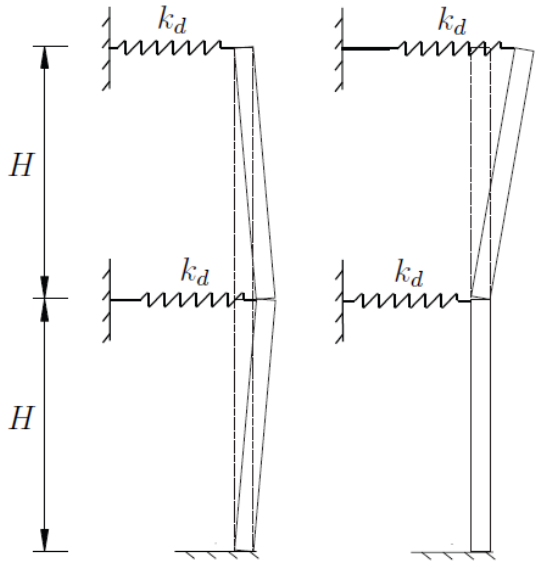

Figure 10: Assumed deformation modes for one-way vertically spanning walls.

$$T_2 = 2\pi\sqrt{\frac{8}{15k^*}(m_d + m_w)} \tag{8}$$

where

$$k^* = 2k_w + k_d \tag{9}$$

and

$$k_d = \frac{16}{3}G_d'\frac{B}{L} \tag{10}$$

The stiffness contribution of the URM end walls is:

$$k_w = \frac{3E_m I_{cr,\ell}}{H_\ell^3} + \frac{3E_m I_{cr,u}}{H_u^3} = 3E_m\left(\frac{I_{cr,\ell}}{H_\ell^3} + \frac{I_{cr,u}}{H_u^3}\right) \tag{11}$$

where I_{cr} is the moment of inertia of the cracked wall section (corresponding to the secant stiffness at 100 mm wall displacement) and can be approximated as $I_{cr} = 0.01\frac{Lt^3}{12}$ or 0.01 times the moment of inertia of the uncracked section (Derakhshan *et al.* 2013). The subscripts $\boldsymbol{\ell}$ and $\boldsymbol{u}$ refer to the lower and upper walls respectively, recognising that both wall height and wall thickness may vary between stories, such that appropriate values of I_{cr} and H should be adopted to account for such variations. For a top-storey wall, $I_{cr,u}$ is taken as zero.

For mid-height diaphragms the ratio of the periods for the two models shown in Figure 9 is obtained as:

$$\frac{T_2}{T_1} = \sqrt{\frac{k_d}{k^*}} = \sqrt{\frac{k_d}{2k_w + k_d}} = \sqrt{\frac{\frac{16}{3}G_d'\frac{B}{L}}{2\times 3E_m\left(\frac{I_{cr,\ell}}{H_\ell^3} + \frac{I_{cr,u}}{H_u^3}\right) + \frac{16}{3}G_d'\frac{B}{L}}} \tag{12}$$

and substituting the cracked moment of inertia and performing further simplification one can obtain:

$$\frac{k_d}{k^*} \cong \frac{\frac{B}{L}}{0.001\left[\left(\frac{t_\ell}{H_\ell}\right)^3 + \left(\frac{t_u}{H_u}\right)^3\right].L.\alpha_1 + \frac{B}{L}} \tag{13}$$

where t_ℓ and t_u are, respectively, the effective wall thickness in the lower and upper storeys and α_1 is the ratio of the masonry Modulus of Elasticity E_m and diaphragm shear stiffness G_d' at 100 mm maximum diaphragm displacement. i.e.

$$\alpha_1 = \frac{E_m}{G_d'} \tag{14}$$

and α_1 has 1/m units. After further simplification k^* can be calculated as:

$$k^* \cong \left[1 + 0.001\left(\frac{t_\ell^3}{H_\ell^3} + \frac{t_u^3}{H_u^3}\right)\frac{L^2}{B}\alpha_1\right]k_d \tag{15}$$

and the stiffness improvement factor (α_w) due to the stiffness of the orthogonal end walls loaded out-of-plane is therefore calculated as:

$$\alpha_w \cong 1 + 0.001\left(\frac{t_\ell^3}{H_\ell^3} + \frac{t_u^3}{H_u^3}\right)\frac{L^2}{B}\frac{E_m}{G_d'} \tag{16}$$

To demonstrate use of the above expression, consider E_m equal to 3 GPa, and G_d' equal to 240 kN/m (i.e. $\alpha_1 = 12500/m$). For a ground storey height of 4.0 m and thickness of 0.350 m and a second storey wall height of 3.6 m and thickness of 0.230 m and a diaphragm length of 10.4 m and depth of 6.5 m the value of α_w is:

$$\alpha_w \cong 1 + 0.001\left(\frac{0.350^3}{4.000^3} + \frac{0.230^3}{3.600^3}\right)\frac{10.4^2}{6.5}\times\frac{3.0\times 10^9}{240\times 10^3} = 1.194 \tag{17}$$

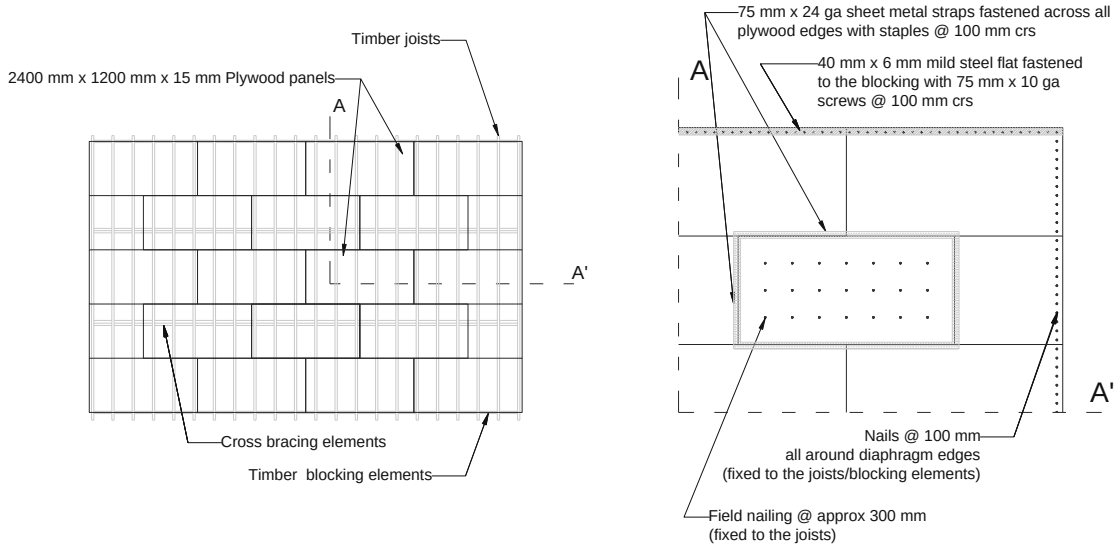

Figure 11: Construction details for a 15 mm plywood overlay solution [Wilson et al. 2014a].

PERIOD OF FLEXIBLE TIMBER DIAPHRAGM

The period T_d of a shear beam having a span L, depth B, effective shear stiffness $G'_{d,eff}$ and loaded with a uniformly distributed tributary weight W_{trib} excited in an approximately parabolic distribution due to the deformation profile of the flexible diaphragm, is given by (Wilson *et al* 2013b, Giongo *et al* 2014):

$$T_d = 0.7 \times \sqrt{\frac{W_{trib} L}{G'_{d,eff} B}} \tag{18}$$

where W_{trib} is the total tributary weight acting on the diaphragm, being the sum of the weight of the tributary walls (ie the product of the tributary height, thickness and density of the two URM walls tributary to the diaphragm accounting for wall penetrations) and diaphragm self-weight plus live load ($\psi_E \times Q_i$ as per NZS 1170.5 section 4.2).

IMPROVED DIAPHRAGMS

Many techniques may be used to improve the performance of flexible timber diaphragms, associated with providing added stiffness and/or strength. The details below specifically pertain to the interpretation of experimental data for improvement techniques that have been physically tested. Improved diaphragms typically exhibit distinct ductility capacity and the results have been interpreted as equivalent elastic-perfectly plastic response, with the reported stiffness being based upon the linear branch of the response curve.

15 mm plywood overlay

Wilson *et al.* (2014a) have reported the performance of newly constructed Pinus radiata flexible diaphragms retrofitted with 15 mm plywood overlays, using the construction details reproduced in Figure 11. Each diaphragm measured 10.4 m × 5.5 m and was comprised of 135 mm × 18 mm straight-edge timber floorboards fastened perpendicular to 45 mm × 290 mm joists spaced at 400 mm centres and oriented along the 5.5 m dimension. The floorboards were fixed to the joists by 3.15 mm × 75 mm common bright roundhead nails driven at a spacing of approximately 95 mm. All retrofits consisted of 2,400 mm × 1,200 mm × 15 mm AS/NZS 2269:2004 structural grade plywood laid over the existing floorboards with 75 mm × 24 gauge sheet metal straps fastened to the plywood edges with ECKO SF-9215 staples at 100 mm centres, as shown in Figure 11. The staple wire had a rectangular cross-section of 1.24 mm × 1.00 mm and a leg length of 15 mm. Field nailing (approximately 300 mm centres) was applied to the plywood sheets at the locations of the joists to mitigate buckling of the panels during large diaphragm displacements, while nailing was provided at 100 mm centres around all diaphragm edges to effectively transfer shear forces. All nails were 3.15 mm (diameter) × 75 mm roundhead power driven nails. Particularly pertinent to later discussion is the orientation of the plywood panels (placed on top of the straight sheathing) and the use of staples at 100 mm centres to fix the sheets to the underlying joists.

The resultant envelopes of the force-displacement response for testing in the directions both parallel and perpendicular to joist orientation are shown in Figure 12, where an averaged bi-linearised response has been overlain for each of the two separate records.

The calculation of diaphragm shear stiffness for each of the 4 retrofitted diaphragms is presented in Table 5, noting that Diaphragm 2b-PARA was tested with a 3.2×1.8 m^2 diaphragm penetration. The symbol Δ_y refers to the bi-linearised yield displacement as plotted in Figure 12.

Substituting the experimental results reported in Table 5 into Equation 4 (accounting for the actual Δ_y given in Table 5 rather than Δ= 0.1 m as written in Equation 4), it may be established that suitable stiffness values for design purposes are: for testing perpendicular to joist G_d = 1,250 kN/m; for testing parallel to joist G_d = 2,400 kN/m. Also, it follows that the ratio of stiffness parallel/perpendicular = 2400/1250 = 1.92.

The general form of the strength equation for improved diaphragms deforming as shear beams is given by:

$$\phi \frac{A_{net}}{A_{gross}} B R_d \geq \frac{F}{2} \tag{19}$$

and hence for the interpretation of experimental results for tested diaphragms (adopting ϕ=1) the unit shear resistance R_d is:

Table 5: Stiffness determination for 15 mm plywood overlay tests by Wilson et al. (2014a)

Description	L (m)	B (m)	F (kN)	Δ_y (m)	$\frac{A_{gross}}{A_{net}}$	G_d (kN/m)
Diaphragm 1b-PERP was tested perpendicular to joists	5.5	10.4	204.7	0.015	1.0	1353
Diaphragm 2b-PERP was tested perpendicular to joists	5.5	10.4	192.6	0.015	1.0	1273
Diaphragm 1b-PARA was tested parallel to joists	10.4	5.5	175.8	0.025	1.0	2493
Diaphragm 2b-PARA was tested parallel to joists with a 3.2×1.8 m^2 penetration	10.4	5.5	171.9	0.025	1.11	2437

Table 6: Strength determination for 15 mm plywood overlay tests by Wilson et al. (2014a)

Description	B (m)	F (kN)	$\frac{A_{gross}}{A_{net}}$	R_d (kN/m)	Δ_y (m)	Δ_u (m)	μ
Diaphragm 1b-PERP was tested perpendicular to joists	10.4	204.7	1.0	9.8	0.015	0.120	8
Diaphragm 2b-PERP was tested perpendicular to joists	10.4	192.6	1.0	9.3	0.015	0.120	8
Diaphragm 1b-PARA was tested parallel to joists	5.5	175.8	1.0	16.0	0.025	0.125	5
Diaphragm 2b-PARA was tested parallel to joists with a 3.2×1.8 m^2 penetration	5.5	171.9	1.11	17.3	0.025	0.125	5

$$R_d \geq \frac{A_{gross}}{A_{net}} \frac{F}{2B} \qquad (20)$$

The calculation of strength values for the diaphragms reported in Figure 12 are presented in Table 6, based upon application of Equation 20. From this data it is concluded that R_d = 9 kN/m is appropriate for loading perpendicular to joists and that R_d = 15 kN/m is appropriate for loading parallel to joists. Also, it follows that the ratio of stiffness parallel/perpendicular = 15/9 = 1.67. The symbol Δ_u is used to describe the maximum displacement achieved before the onset of strength loss due to plastic deformations.

A final feature of the data reported in Figure 12 is that the retrofitted diaphragms had substantial ductility capacity. Whilst larger ductility values were measured for loading oriented perpendicular to joists, it is suggested that the lowest measured value be applied for both loading orientations. As shown in Table 6 it is concluded that the 15 mm plywood overlay had a reliable displacement ductility of μ = 5. A conservative value of μ = 4 has been adopted.

The improvement in diaphragm response associated with the 15 mm plywood overlay is shown in Figure 13, where it can be clearly seen that the retrofit solution resulted in a substantial increase in both shear stiffness and shear strength.

Ceiling sheathing and tin ceiling lining

One scenario that is routinely encountered in vintage flexible timber diaphragms in New Zealand is the presence of a patterned tin ceiling lining covering a sheathed ceiling diaphragm (see Figure 14). This diaphragm detailing was investigated by testing Diaphragm A (refer to Table 1) both with and without the combination of the ceiling lining and tin ceiling overlay.

When comparing the data reported in Figure 15(b) it can be determined that the combination of ceiling sheathing and tin ceiling lining significantly influenced both the strength and stiffness characteristics of the diaphragm and therefore this

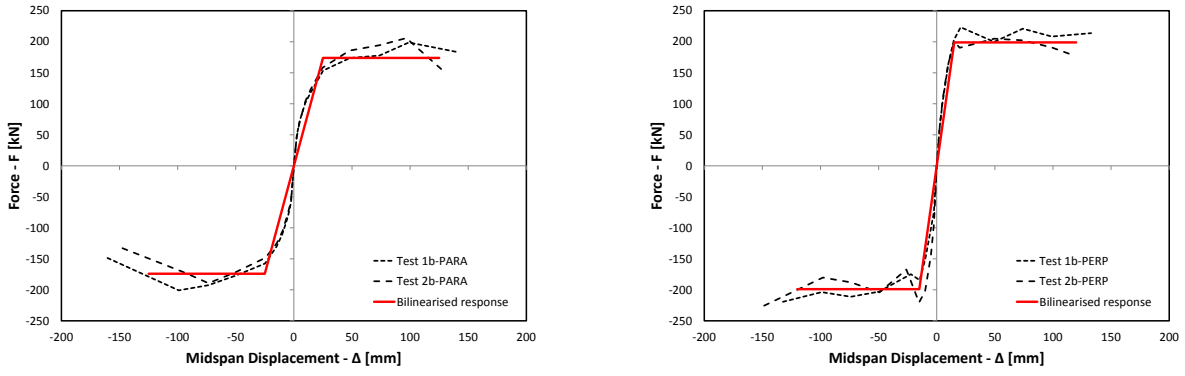

(a) Loading parallel to joist *(b) Loading perpendicular to joist*

Figure 12: Force-displacement response of newly constructed diaphragms retrofitted with a 15 mm plywood overlay [Wilson et al. 2014a].

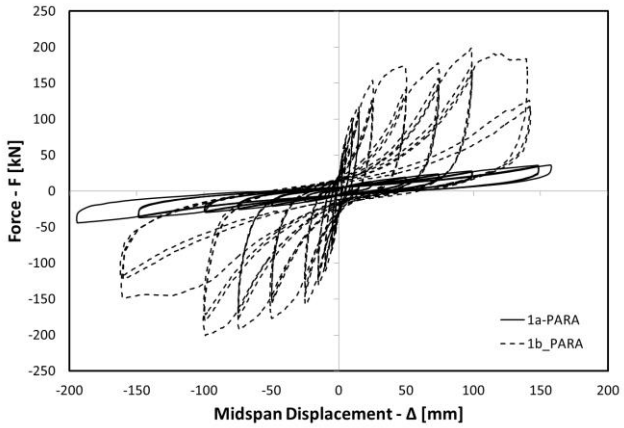

(a) Diaphragms 1a-PARA and 1b-PARA.

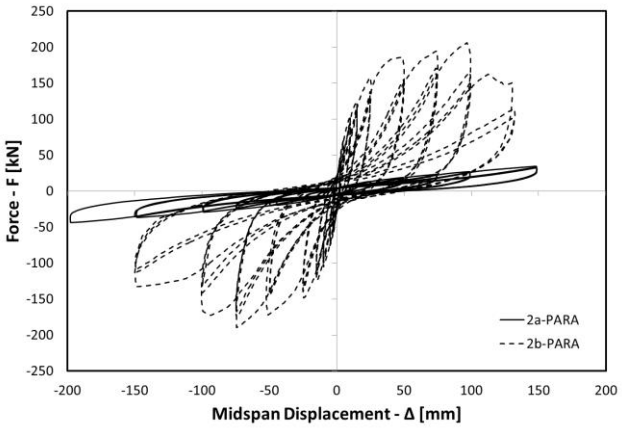

(b) Diaphragms 2a-PARA and 2b-PARA.

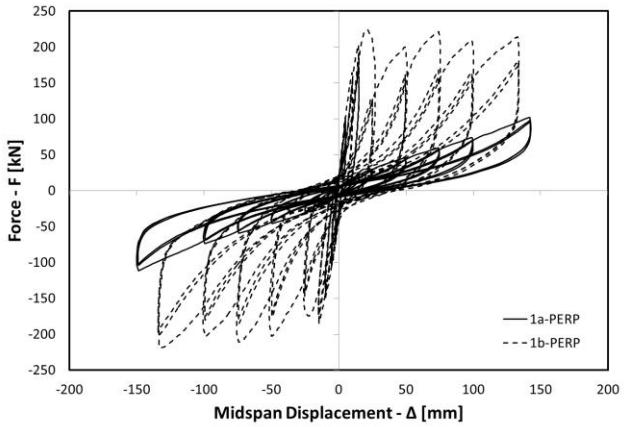

(c) Diaphragms 1a-PERP and 1b-PERP.

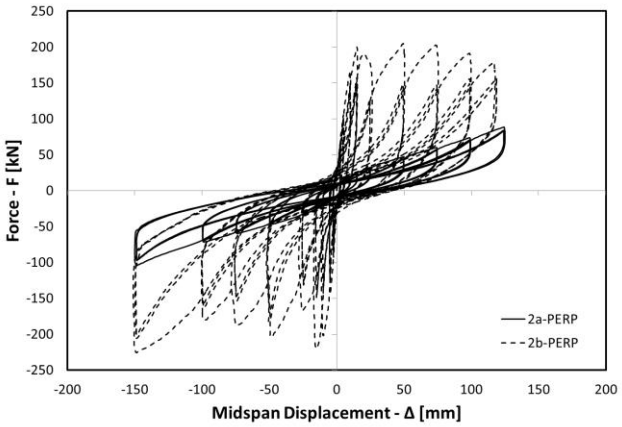

(d) Diaphragms 2a-PERP and 2b-PERP.

Figure 13: Comparison of force-displacement response for diaphragms tested as-built and after being retrofitted with a 15 mm plywood overlay [Wilson et al. 2014a].

diaphragm configuration is considered to be a diaphragm improvement, even if the configuration was part of the original construction.

The data used to establish the stiffness of the diaphragm having straight sheathed floorboards and a straight sheathed ceiling combined with a 0.3 mm patterned tin ceiling lining is shown in
reports the shear stiffness of diaphragm A when having both the flooring and ceiling sheathing present, plus the tin ceiling lining.

From Figure 15(a) it can be established that diaphragm A with an added straight sheathed ceiling diaphragm and a patterned tin ceiling lining had R_d = 75/2/5.6 = 6.7 kN/m and a ductility capacity of μ = 2.

When inspecting the data shown in Figure 15(b) it can be established that for the tolerable range of diaphragm mid-span displacements (generally less than approximately 100 mm) the single straight sheathed diaphragm exhibits an approximately elastic response (admittedly with some loss in stiffness on load reversal) whereas the presence of the added ceiling sheathing and ceiling lining results in a response that exhibits a strength plateau and is therefore distinctly nonlinear.

As testing of the diaphragm with ceiling sheathing and patterned tin ceiling lining was not undertaken for loading oriented parallel to joist, the relationships determined previously for the testing undertaken by Wilson *et al.* (2014a) were applied to forecast the stiffness and strength parameters for the orthogonal direction of loading. Adopting G_d = 950 kN/m for stiffness in the direction perpendicular to joists

Figure 14: Patterned 0.3 mm tin ceiling lining underlying a straight sheathed flexible timber ceiling diaphragm.

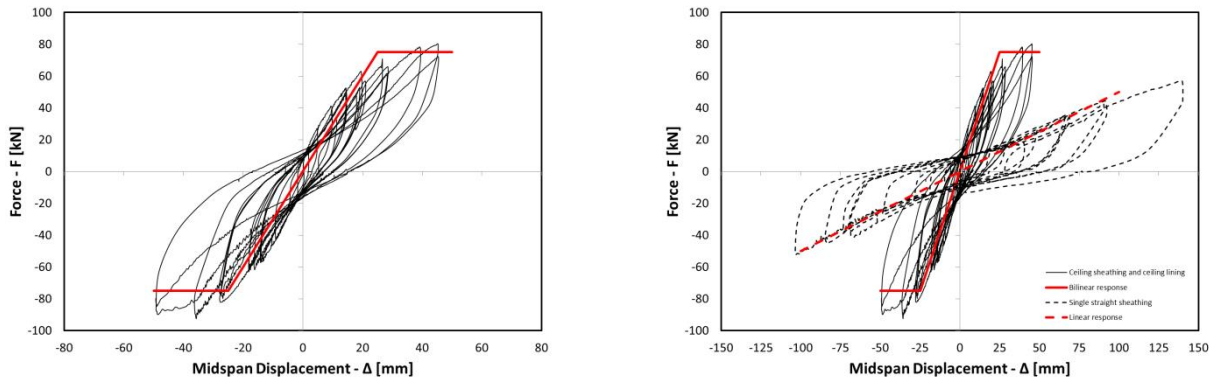

(a) With ceiling sheathing and tin ceiling lining.

(b) Comparison with and without diaphragm ceiling improvements.

Figure 15: Force-displacement response of diaphragm A with and without added ceiling sheathing and patterned tin ceiling lining.

Table 7: Secant stiffness values for in-situ testing of vintage diaphragm loaded perpendicular to joists

Description	L (m)	B (m)	F (kN)	Δ_y (m)	G_d (kN/m)
Diaphragm A with sheathed ceiling lining and patterned tin ceiling overlay (see Figure 15(a)). Refer to Table 1 for the equivalent response without the sheathed ceiling lining and tin ceiling overlay	9.6	5.6	75.0	0.025	964

and applying the ratio of 1.92 found from the Wilson *et al.* (2014a) testing, the projected stiffness is approximately G_d = 1,800 kN/m for loading parallel to joist. Similarly, adopting R_d = 6.5 kN/m for loading perpendicular to joists and applying the ratio of 1.67 found from the Wilson *et al.* (2014a) testing, the projected strength is approximately R_d = 10.5 kN/m for loading oriented parallel to joists.

9 mm plywood overlay

Giongo *et al.* (2013) instituted a 9 mm plywood overlay retrofit when testing the diaphragm in the building located in Whanganui, with specific detailing as shown in Figure 16. Attention is drawn to the symmetrical orientation of the plywood panels, resulting in isotropic rather than orthotropic diaphragm strength characteristics, and the use of gage 6 screws (30 mm long) to fix panels to the underlying flooring only, rather than attempting to fix the overlay through the flooring and into the joists. This fixing strategy eliminated the need to cut the diaphragm panels to match the joist spacing, other than on the diaphragm perimeter. Diaphragm to wall shear transfer was provided by the gage 8 screws (60 mm long) installed on the diaphragm perimeter.

When comparing the data in Table 8 with the comparable data in Table 5 for testing oriented perpendicular to joist, it would initially seem unusual that the 9 mm ply overlay was stiffer than the 15 mm ply overlay. The explanation comes from recognising that the orientation of the plywood panels was more advantageous for the configuration shown in Figure 16 and that the use of screws rather than nails resulted in stiffer connections. Conversely, as the configuration shown in Figure 16 is symmetrical the same G_d value is adopted for both loading directions. Hence when comparing the stiffness ratios for the direction parallel to joist of 2,400 kN/m and

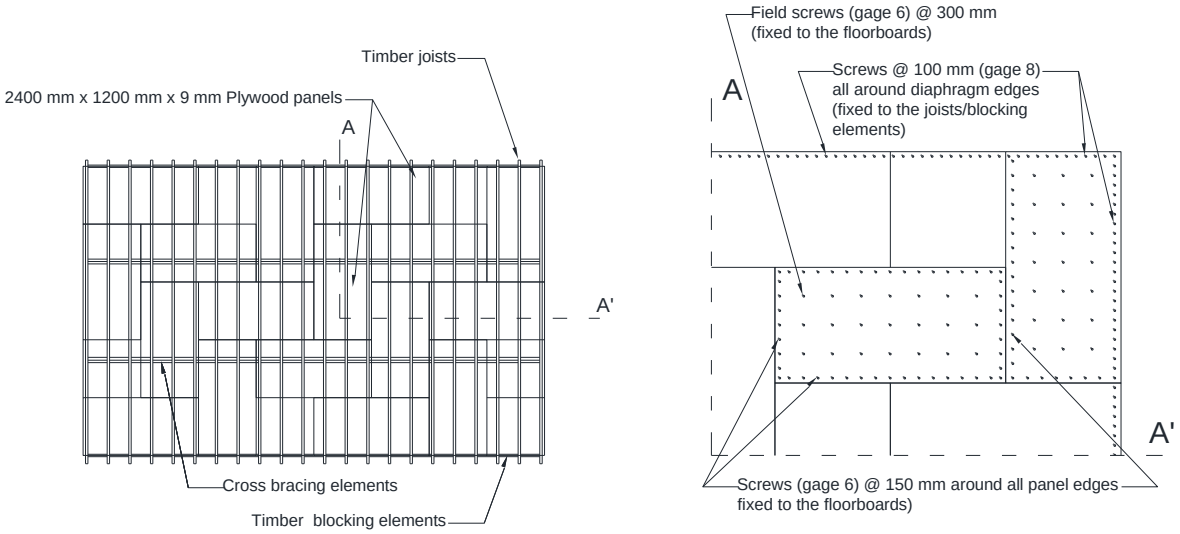

Figure 16: Construction details of a 9 mm plywood overlay solution [Giongo et al. 2013].

Table 8: Secant stiffness determination for 9 mm plywood overlay test by Giongo et al. (2013)

Description	L (m)	B (m)	F (kN)	Δ_y (m)	G_d (kN/m)
Diaphragm B with 9 mm plywood overlay tested perpendicular to joists (see Figure 16). Note that the diaphragm depth for this test was reduced to 2.8 m due to limited capacity of the loading system and increased capacity of the diaphragm retrofit.	9.6	2.8	96	0.042	1469

1,460 kN/m for the 15 mm and 9 mm plywood overlays respectively, it is found that 2400/1460 = 1.64 whereas 15/9 = 1.67, suggesting that for loading oriented parallel to joists the plywood thickness might be directly responsible for dictating the overall diaphragm shear stiffness.

The shear strength of the 9 mm plywood overlay is defined by R_d = 96/2/2.8 = 17.1 kN/m. Because the diaphragm configuration is symmetrical the strength is also assumed to be symmetrical in both directions and a conservative strength of 16.0 kN/m is assumed. Because the testing was terminated before any signs of distress were evident, it is conservatively assumed that the design has a ductility capacity of $\mu = 3$.

Summary of shear stiffness and strength values for diaphragm improvements

The data presented above pertaining to experimentally tested diaphragm improvement techniques is summarised in Table 9.

CONCLUSIONS

A systematic approach to the detailed seismic assessment of vintage New Zealand flexible timber diaphragms is presented, incorporating all available field test data and integrating with the existing ASCE 41-13 technique when field test data is unavailable. Three tested improvement techniques were presented with a view to these results forming the basis for standard detailing. The intent is that the procedure may be further refined and developed as additional test data becomes available.

The main differences introduced in the proposed approach, when compared with procedures presented elsewhere, are the selection of the critical diaphragm displacement being dependent on out-of-plane URM end wall deformations, and the use of this criterion to establish the diaphragm secant shear stiffness. A procedure to account for possible degradation of the diaphragms is also presented.

The presented procedure is based upon developing a suitably accurate elastic procedure whilst recognising that diaphragm response can be highly nonlinear. For diaphragm configurations outside those considered here, the use of nonlinear modelling may be necessary to establish probable diaphragm deformation response (Wilson 2012). Similarly, designers should consider undertaking a sensitivity analysis to establish the extent of variation in response that is derived from assumptions regarding diaphragm condition.

An application of the proposed approach to a case study is reported in Appendix A.

ACKNOWLEDGEMENTS

The field testing in Whanganui reported herein was undertaken with funding provided by the New Zealand Natural Hazards Research Platform. Giongo received partial financial support for this study from the Italian RELUIS Consortium, within the 2010-2012 research program carried out for the Italian Agency for Emergency Management. Wilson's research was undertaken via a Tertiary Education Commission Bright Futures scholarship and funding provided by the Foundation for Research Science and Technology. The authors wish to thank Jitendra Bothara, Rob Jury, Lou Robinson, Stefano Pampanin, Alistair Cattanach and Stuart Oliver for their assistance in developing the methodology presented herein, as part of their efforts on the NZSEE study group addressing detailed seismic assessment of URM buildings. Gye Simkin is thanked for the preparation of many of the diagrams included herein.

REFERENCES

1. Agbabian & Associates, S. B. Barnes & Associates, and Kariotis & Associates, (ABK) A Joint Venture. (1982). 'Methodology for mitigation of seismic hazards in existing unreinforced masonry buildings: Interpretation of diaphragm tests', Rep. No. ABK-TR-05, El Segundo, Calif.
2. ANSI/ASME B18.6.1-1981 (R2008) 'Wood Screws', American Society of Mechanical Engineers, New York, NY.

Table 9: Shear stiffness values for diaphragm improvement techniques

Description of diaphragm improvement	Shear stiffness, G_d (kN/m)		Shear strength, R_d (kN/m)		Ductility†, μ
	Parallel to joist	Perpendicular to joist	Parallel to joist	Perpendicular to joist	
Straight sheathed flooring plus straight sheathed ceiling with patterned tin ceiling lining	1800	950	10.5	6.5	2
9 mm plywood panel overlay (blocked, unchorded, see Figure 16)	1460	1460	16.0	16.0	3
Straight sheathed flooring plus 15 mm plywood panel overlay (see Figure 11)	2400	1250	15.0	9.0	4

† Care must be exercised on the appropriate specification of wood screws when ductile diaphragm response is adopted. Appropriate wood screws to ensure ductile response include those manufactured in accordance with EN 14592 and having a CE mark and those manufactured in accordance with B18.6.1-1981 (R2008) from ASME (American Society of Mechanical Engineers).

3. AS/NZS 2269:2004, Plywood – Structural, Standard New Zealand.
4. ASCE 41-13 (2013). 'Seismic evaluation and retrofit of existing buildings', American Society of Civil Engineers, Reston, Virginia.
5. Brignola, A., Pampanin, S., Podestà, S. (2012). 'Experimental Evaluation of the In-Plane Stiffness of Timber Diaphragms', *Earthquake Spectra,* **28**(4), 1687-1709.
6. BS EN 14592:2008, Timber structures – Dowel-type fasteners – Requirements, 2008 (Plus amendment 1 2012), British Standards Institution, London, UK, BSI.
7. Derakhshan, H., Griffith, M. C., Ingham, J. M. (2013). 'Out-of-plane behaviour of one-way spanning URM walls', *ASCE Journal of Engineering Mechanics*, **139**(4), 409-417.
8. Faconni, L., Plizzari, G., Vecchio, F. (2013). 'Disturbed stress field model for unreinforced masonry', *ASCE Journal of Structural Engineering*, **140**(4), 04013085.
9. Giongo, I., Dizhur, D., Tomasi, R., Ingham, J. M. (2013). 'In-plane assessment of existing timber diaphragms in URM buildings via quasi-static and dynamic in-situ tests', *Advanced Materials Research*, **778**, 495-502.
10. Giongo, I., Dizhur, D., Tomasi, R., Ingham, J. M. (2014). 'Field testing of flexible timber diaphragms in an existing vintage URM building', ASCE Journal of Structural Engineering, In Press, DOI: 10.1061/(ASCE)ST.1943-541X.0001045.
11. Griffith, M. C., Vaculik, J., Lam, N. T. K., Wilson, J., Lumantarna, E. (2007). 'Cyclic testing of unreinforced masonry walls in two-way bending', *Earthquake Engineering and Structural Dynamics,* **36**(6), 801-821.
12. Kent, S. M., Leichti, R. J., Rosowsky, D. V., Morrell, J. J. (2005). 'Effects of decay on the cyclic properties of nailed connections', *ASCE Journal of Materials in Civil Engineering,* **17**(5), 57-585.
13. Magenes, G., Kingsley, Calvi, G. M. (1995). 'Seismic testing of a full-scale, two-storey masonry building: test procedure and measured experimental response', Report 3.0, CNR-GNDT, Italy.
14. New Zealand Society for Earthquake Engineering, (2006). 'Assessment and improvement of the structural performance of buildings in earthquakes', Recommendations of a NZSEE study group on earthquake risk buildings, Wellington.
15. NZS 1170.5 (2004). 'Structural design actions, Part 5: Earthquake actions – New Zealand', *Standards New Zealand*, Wellington.
16. Ragget, J. D., Rojahn, C. (1991). 'Dynamic amplification of ground motion by low-rise, stiff shear wall buildings', SMIP91 Seminar on Seismological and Engineering Implications of Recent Strong-Motion Data, Preprints, *California Division of Mines and Geology*, Sacramento, 1-11.
17. Sawata, K., Sasaki, T., Doi, S., Iijima, Y. (2008). 'Effect of decay on shear performance of dowel-type timber joints', *The Journal of Wood Science*, **54**, pp. 356-361.
18. Tena Colunga, A., Abrams, D. P. (1996). 'Seismic Behavior of Structures with Flexible Diaphragms', *ASCE Journal of Structural Engineering*, **122**(4), pp. 439-445.
19. Vaculik, J. (2012). 'Unreinforced masonry walls subjected to out-of-plane seismic actions', Doctoral dissertation, University of Adelaide.
20. Wilson, A. (2012).' Seismic assessment of timber floor diaphragms in unreinforced masonry buildings', Doctoral dissertation, The University of Auckland, Auckland, New Zealand, March, 568p. https://researchspace.auckland.ac.nz/handle/2292/14696
21. Wilson, A., Kelly, P. A., Quenneville, P. J. H., Ingham, J. M. (2013a). 'Non-linear in-plane deformation mechanics of timber floor diaphragms in unreinforced masonry buildings', *ASCE Journal of Engineering Mechanics,* **140**(4), 04013010.
22. Wilson, A., Quenneville, P., Ingham, J. (2013b). 'Natural Period and Seismic Idealization of Flexible Timber Diaphragms', *Earthquake Spectra,* **29**(3), 1003-1019.
23. Wilson, A., Quenneville, P. J. H., Ingham, J. M. (2014a). 'In-plane orthotropic behaviour of timber floor diaphragms in unreinforced masonry buildings', *ASCE Journal of Structural Engineering,* **140**(1), 04013038.
24. Wilson, A., Quenneville, P. J. H., Moon, F. L., Ingham, J. M. (2014b). 'Lateral performance of nail connections from century old timber floor diaphragms', *ASCE Journal of Materials in Civil Engineering*, **26**(1), 202-205.

APPENDIX A: ASSESSMENT EXAMPLE FOR FLEXIBLE TIMBER DIAPHRAGMS

A 2-storey unreinforced masonry building has a ground floor height of 4.0 m with 3 leaf (305 mm) wall thickness and a second storey height of 3.6 m with 2 leaf (210 mm) wall thickness. The overall plan dimensions of the building are 8.5 m × 12.8 m. The long axis of the building is aligned parallel to the street and the front face of the building has regular penetrations while all other walls are solid. The ground floor wall facing the street has 85% of the surface as penetrations and the second floor wall has 50% of the wall surface as penetrations. The building has a parapet of height 2.0 m on the street frontage with height of 0.8 m on other sides. The masonry has an assessed Modulus of Elasticity of 3.0 GPa.

The mid-height floor diaphragm sits on a ledge and is securely connected to all perimeter walls. The joists span the short dimension of the building, and are discontinuous but spliced with a reliable mechanical anchorage. The mid-height floor diaphragm is straight sheathed, is rated to be in fair condition, and has a penetration of 1.2 m × 3.5 m. The ceiling diaphragm is single diagonally sheathed with no chord, has discontinuous joists with reliable anchorage, and is in poor condition. Diaphragm sheathing is 18 mm thick and joists are 55 × 240 mm spaced at 405 mm centres. A timber density of 610 kg/m^3 is used, corresponding to a mid-height floor diaphragm self weight of 0.3 kN/m^2. The self-weight of the ceiling diaphragm including roof coverings and trusses is taken as 0.6 kN/m^2. Masonry density is assumed to be 1,800 kg/m^3.

The building is located in Gisborne on soft soil (site subsoil class C). The building contains general office space (occupancy type B, Q = 3 kPa).

For response parallel to joist

	Floor (subscript f)	Ceiling (subscript c)
Condition Rating	$fair$	$poor$
Default Shear Stiffness (Table 3)	$K_f := 285\ \frac{kN}{m}$	$K_c := 225\ \frac{kN}{m}$
Sheathing Multiplier (Table 4)	$\alpha_{sf} := 1$	$\alpha_{sc} := 2$
Overall Building Length	$L_T := 12.8\ m$	
Perpendicular wall thickness at diaphragm height for length dimension	$t_{Lf} := 0.21\ m$	$t_{Lc} := 0.21\ m$
Diaphragm span for loading oriented parallel to joist	$L_f := L_T - 2 \cdot t_{Lf} = 12.38\ m$	$L_c := L_T - 2 \cdot t_{Lc} = 12.38\ m$
Overall building width	$W := 8.5\ m$	
Perpendicular wall thickness at diaphragm height for width dimension	$t_{Wf} := 0.21\ m$	$t_{Wc} := 0.21\ m$
Diaphragm depth for loading oriented parallel to joist	$B_f := W - 2 \cdot t_{Wf} = 8.08\ m$	$B_c := W - 2 \cdot t_{Wc} = 8.08\ m$
Diaphragm gross area	$A_{gf} := L_f \cdot B_f = 100.03\ m^2$	$A_{gc} := L_c \cdot B_c = 100.03\ m^2$
Diaphragm penetration area	$A_{pf} := 1.2\ m \cdot 3.5\ m = 4.2\ m^2$	$A_{pc} := 0\ m^2$
Penetration factor	$\alpha_{pf} := \frac{\langle A_{gf} - A_{pf} \rangle}{A_{gf}} = 0.958$	$\alpha_{pc} := \frac{\langle A_{gc} - A_{pc} \rangle}{A_{gc}} = 1$
Shear stiffness	$G'_{df} := \alpha_{pf} \cdot \alpha_{sf} \cdot K_f = 273.03\ \frac{kN}{m}$	
	$G'_{dc} := \alpha_{pc} \cdot \alpha_{sc} \cdot K_c = 450\ \frac{kN}{m}$	

Thickness of wall below diaphragm $t_{lf} := 0.305\ m$ $t_{lc} := 0.21\ m$

Height of wall below diaphragm $H_{lf} := 4\ m$ $H_{lc} := 3.6\ m$

Thickness of wall above diaphragm $t_{uf} := t_{Wf} = 0.21\ m$ $t_{uc} := 0\ m$

Height of wall above diaphragm $H_{uf} := 3.6\ m$ $H_{uc} := 0\ m$

Masonry modulus of elasticity $E_m := 3\ GPa$

Wall stiffness multiplier

$$\alpha_{wf} := 1 + \left[\left(\frac{t_{lf}}{H_{lf}}\right)^3 + \left(\frac{t_{uf}}{H_{uf}}\right)^3\right] \cdot \frac{L_f^{\,2}}{B_f} \cdot \frac{E_m}{G'_{df}} \cdot \frac{1}{1000} = 1.134$$

$$\alpha_{wc} := 1 + \left(\frac{t_{lc}}{H_{lc}}\right)^3 \cdot \frac{L_c^{\,2}}{B_c} \cdot \frac{E_m}{G'_{dc}} \cdot \frac{1}{1000} = 1.025$$

Effective shear stiffness

$$G'_{deff\_f} := \alpha_{wf} \cdot G'_{df} = 309.56\ \frac{kN}{m}$$

$$G'_{deff\_c} := \alpha_{wc} \cdot G'_{dc} = 461.3\ \frac{kN}{m}$$

Mass density of masonry $\rho_m := 1800\ \frac{kg}{m^3}$

Volume of tributary masonry per unit length (2 walls)

- % penetrations in wall 1 lower storey	$p_{1lf} := 85\%$	$p_{1lc} := 50\%$
- % penetrations in wall 1 upper storey	$p_{1uf} := 50\%$	$p_{1uc} := 0\%$
- % penetrations in wall 2 lower storey	$p_{2lf} := 0\%$	$p_{2lc} := 0\%$
- % penetrations in wall 2 upper storey	$p_{2uf} := 0\%$	$p_{2uc} := 0\%$
- Tributary height of wall 1 below diaphragm	$H_{t1lf} := \frac{H_{lf}}{2} = 2\ m$	$H_{t1lc} := \frac{H_{lc}}{2} = 1.8\ m$
- Tributary height of wall 1 above diaphragm (include parapet)	$H_{t1uf} := 1.8\ m$	$H_{t1uc} := 2\ m$
- Tributary height of wall 2 below diaphragm	$H_{t2lf} := 2\ m$	$H_{t2lc} := 1.8\ m$
- Tributary height of wall 2 above diaphragm (include parapet)	$H_{t2uf} := 1.8\ m$	$H_{t2uc} := 0.8\ m$

$V_{uf} := L_f \cdot t_{Lf} \cdot \left(\left(1 - p_{1uf}\right) \cdot H_{t1uf} + \left(1 - p_{2uf}\right) \cdot H_{t2uf} \right) = 7.019\ m^3$

$V_{lf} := L_f \cdot t_{lf} \cdot \left(\left(1 - p_{1lf}\right) \cdot H_{t1lf} + \left(1 - p_{2lf}\right) \cdot H_{t2lf} \right) = 8.685\ m^3$

$V_{uc} := L_c \cdot t_{Lc} \cdot \left(\left(1 - p_{1uc}\right) \cdot H_{t1uc} + \left(1 - p_{2uc}\right) \cdot H_{t2uc} \right) = 7.279\ m^3$

$V_{lc} := L_c \cdot t_{lc} \cdot \left(\left(1 - p_{1lc}\right) \cdot H_{t1lc} + \left(1 - p_{2lc}\right) \cdot H_{t2lc} \right) = 7.019\ m^3$

Weight of walls

$W_f := \rho_m \cdot \left(9.81\ \frac{m}{s^2} \right) \left(V_{uf} + V_{lf} \right) = 277.3\ kN$

$W_c := \rho_m \cdot \left(9.81\ \frac{m}{s^2} \right) \left(V_{uc} + V_{lc} \right) = 252.49\ kN$

Self weight area loading

$w_f := 0.3\ kPa$ $w_c := 0.6\ kPa$

Self weight

$P_{wf} := w_f \cdot A_{gf} \cdot \alpha_{pf} = 28.75\ kN$

$P_{wc} := w_c \cdot A_{gc} \cdot \alpha_{pc} = 60.02\ kN$

Imposed action area loading

$q_f := 3\ kPa$ $q_c := 0\ kPa$

Area reduction factor

$\omega_f := 0.3 + \frac{3}{\sqrt{\alpha_{pf} \cdot A_{gf}}} = 0.606$

Imposed weight

$P_{qf} := 0.3 \cdot q_f \cdot \omega_f \cdot \alpha_{pf} \cdot A_{gf} = 52.31\ kN$

Total tributary weight

$W_{Tf} := W_f + P_{wf} + P_{qf} = 358.4\ kN$

$W_{Tc} := W_c + P_{wc} = 312.51\ kN$

Period

$T_f := 0.7 \cdot \sqrt{\frac{W_{Tf} \cdot L_f}{G'_{deff\_f} \cdot B_f}} = 0.93\ sec$

$T_c := 0.7 \cdot \sqrt{\frac{W_{Tc} \cdot L_c}{G'_{deff\_c} \cdot B_c}} = 0.71\ sec$

Critical displacement at 2.5% drift

$d_{cri\_f} := 2.5\% \cdot H_{t1lf} \cdot 2 = 100\ mm$

$d_{cri\_c} := 2.5\% \cdot H_{t1lc} \cdot 2 = 90\ mm$

Site hazard coefficient to match acceptance criteria

$C_f := \left(\frac{16}{3} \right) \cdot \frac{G'_{deff\_f} \cdot B_f \cdot d_{cri\_f}}{W_{Tf} \cdot L_f} = 0.3$

$C_c := \left(\frac{16}{3} \right) \cdot \frac{G'_{deff\_c} \cdot B_c \cdot d_{cri\_c}}{W_{Tc} \cdot L_c} = 0.46$

Code factors

$Z := 0.36$ $R := 1$ $N(T, D) := 1$

$C_{h\_f} := 1.34$ $C_{h\_c} := 1.61$

Actual site hazard coefficient
NZS 1170.5 Eq 3.1(1)

$C_{act\_f} := Z \cdot R \cdot N(T, D) \cdot C_{h\_f} = 0.48$

$C_{act\_c} := Z \cdot R \cdot N(T, D) \cdot C_{h\_c} = 0.58$

%NBS for diaphragms

$P_{NBS\_f} := \frac{C_f}{C_{act\_f}} = 62\%$ $P_{NBS\_c} := \frac{C_c}{C_{act\_c}} = 80\%$

Forecast diaphragm displacement at design loading

$d_{for\_f} := \left(\frac{3}{16}\right) \cdot \frac{C_{act\_f} \cdot W_{Tf} \cdot L_f}{B_f \cdot G'_{deff\_f}} = 160\ mm$

$d_{for\_c} := \left(\frac{3}{16}\right) \cdot \frac{C_{act\_c} \cdot W_{Tc} \cdot L_c}{B_c \cdot G'_{deff\_c}} = 113\ mm$

For response perpendicular to joist

	Floor (subscript f)	Ceiling (subscript c)
Condition Rating	*fair*	*poor*
Default Shear Stiffness (Table 3)	$K_f := 215\ \frac{kN}{m}$	$K_c := 170\ \frac{kN}{m}$
Sheathing Multiplier (Table 4)	$\alpha_{sf} := 1$	$\alpha_{sc} := 2$
Overall Building Length	$L_T := 8.5\ m$	
Perpendicular wall thickness at diaphragm height for length dimension	$t_{Lf} := 0.21\ m$	$t_{Lc} := 0.21\ m$
Diaphragm span for loading oriented parallel to joist	$L_f := L_T - 2 \cdot t_{Lf} = 8.08\ m$	$L_c := L_T - 2 \cdot t_{Lc} = 8.08\ m$
Overall building width	$W := 12.8\ m$	
Perpendicular wall thickness at diaphragm height for width dimension	$t_{Wf} := 0.21\ m$	$t_{Wc} := 0.21\ m$
Diaphragm depth for loading oriented parallel to joist	$B_f := W - 2 \cdot t_{Wf} = 12.38\ m$	$B_c := W - 2 \cdot t_{Wc} = 12.38\ m$
Diaphragm gross area	$A_{gf} := L_f \cdot B_f = 100.03\ m^2$	$A_{gc} := L_c \cdot B_c = 100.03\ m^2$
Diaphragm penetration area	$A_{pf} := 1.2\ m \cdot 3.5\ m = 4.2\ m^2$	$A_{pc} := 0\ m^2$
Penetration factor	$\alpha_{pf} := \frac{\langle A_{gf} - A_{pf} \rangle}{A_{gf}} = 0.96$	$\alpha_{pc} := \frac{\langle A_{gc} - A_{pc} \rangle}{A_{gc}} = 1$
Shear stiffness	$G'_{df} := \alpha_{pf} \cdot \alpha_{sf} \cdot K_f = 205.97\ \frac{kN}{m}$	
	$G'_{dc} := \alpha_{pc} \cdot \alpha_{sc} \cdot K_c = 340\ \frac{kN}{m}$	

Thickness of wall below diaphragm $t_{lf} := 0.305\ m$ $t_{lc} := 0.21\ m$

Height of wall below diaphragm $H_{lf} := 4\ m$ $H_{lc} := 3.6\ m$

Thickness of wall above diaphragm $t_{uf} := t_{Wf} = 0.21\ m$ $t_{uc} := 0\ m$

Height of wall above diaphragm $H_{uf} := 3.6\ m$ $H_{uc} := 0\ m$

Masonry modulus of elasticity $E_m := 3\ GPa$

Wall stiffness multiplier

$$\alpha_{wf} := 1 + \left[\left(\frac{t_{lf}}{H_{lf}}\right)^3 + \left(\frac{t_{uf}}{H_{uf}}\right)^3\right] \cdot \frac{L_f^{\,2}}{B_f} \cdot \frac{E_m}{G'_{df}} \cdot \frac{1}{1000} = 1.049$$

$$\alpha_{wc} := 1 + \left(\frac{t_{lc}}{H_{lc}}\right)^3 \cdot \frac{L_c^{\,2}}{B_c} \cdot \frac{E_m}{G'_{dc}} \cdot \frac{1}{1000} = 1.009$$

Effective shear stiffness

$$G'_{deff\_f} := \alpha_{wf} \cdot G'_{df} = 216.13\ \frac{kN}{m}$$

$$G'_{deff\_c} := \alpha_{wc} \cdot G'_{dc} = 343.14\ \frac{kN}{m}$$

Mass density of masonry $\rho_m := 1800\ \frac{kg}{m^3}$

Volume of tributary masonry per unit length (2 walls)

- % penetrations in wall 1 lower storey $p_{1lf} := 0\%$ $p_{1lc} := 0\%$
- % penetrations in wall 1 upper storey $p_{1uf} := 0\%$ $p_{1uc} := 0\%$
- % penetrations in wall 2 lower storey $p_{2lf} := 0\%$ $p_{2lc} := 0\%$
- % penetrations in wall 2 upper storey $p_{2uf} := 0\%$ $p_{2uc} := 0\%$

- Tributary height of wall 1 below diaphragm $H_{t1lf} := \frac{H_{lf}}{2} = 2\ m$ $H_{t1lc} := \frac{H_{lc}}{2} = 1.8\ m$
- Tributary height of wall 1 above diaphragm (include parapet) $H_{t1uf} := 1.8\ m$ $H_{t1uc} := 0.8\ m$
- Tributary height of wall 2 below diaphragm $H_{t2lf} := 2\ m$ $H_{t2lc} := 1.8\ m$
- Tributary height of wall 2 above diaphragm (include parapet) $H_{t2uf} := 1.8\ m$ $H_{t2uc} := 0.8\ m$

$$V_{uf} := L_f \cdot t_{Lf} \cdot \langle (1 - p_{1uf}) \cdot H_{t1uf} + (1 - p_{2uf}) \cdot H_{t2uf} \rangle = 6.108\ m^3$$

$$V_{lf} := L_f \cdot t_{lf} \cdot \langle (1 - p_{1lf}) \cdot H_{t1lf} + (1 - p_{2lf}) \cdot H_{t2lf} \rangle = 9.858\ m^3$$

$$V_{uc} := L_c \cdot t_{Lc} \cdot \langle (1 - p_{1uc}) \cdot H_{t1uc} + (1 - p_{2uc}) \cdot H_{t2uc} \rangle = 2.715\ m^3$$

$$V_{lc} := L_c \cdot t_{lc} \cdot \langle (1 - p_{1lc}) \cdot H_{t1lc} + (1 - p_{2lc}) \cdot H_{t2lc} \rangle = 6.108\ m^3$$

Weight of walls

$$W_f := \rho_m \cdot \left(9.81\ \frac{m}{s^2}\right) \langle V_{uf} + V_{lf} \rangle = 281.93\ kN$$

$$W_c := \rho_m \cdot \left(9.81\ \frac{m}{s^2}\right) \langle V_{uc} + V_{lc} \rangle = 155.8\ kN$$

Self weight area loading $w_f := 0.3\ kPa$ $w_c := 0.6\ kPa$

Self weight

$$P_{wf} := w_f \cdot A_{gf} \cdot \alpha_{pf} = 28.75\ kN$$

$$P_{wc} := w_c \cdot A_{gc} \cdot \alpha_{pc} = 60.02\ kN$$

Imposed action area loading $q_f := 3\ kPa$ $q_c := 0\ kPa$

Area reduction factor $$\omega_f := 0.3 + \frac{3}{\sqrt{\alpha_{pf} \cdot A_{gf}}} = 0.606$$

Imposed weight $$P_{qf} := 0.3 \cdot q_f \cdot \omega_f \cdot \alpha_{pf} \cdot A_{gf} = 52.31\ kN$$

Total tributary weight

$$P_{Tf} := W_f + P_{wf} + P_{qf} = 363\ kN$$

$$P_{Tc} := W_c + P_{wc} = 215.82\ kN$$

Period $$T_f := 0.7 \cdot \sqrt{\frac{P_{Tf} \cdot L_f}{G'_{deff\_f} \cdot B_f}} = 0.73\ sec$$

$$T_c := 0.7 \cdot \sqrt{\frac{P_{Tc} \cdot L_c}{G'_{deff\_c} \cdot B_c}} = 0.45\ sec$$

Critical displacement at 2.5% drift $d_{cri\_f} := 2.5\% \cdot H_{t1lf} \cdot 2 = 100\ mm$

$$d_{cri\_c} := 2.5\% \cdot H_{t1lc} \cdot 2 = 90\ mm$$

Site hazard coefficient to match acceptance criteria

$$C_f := \left(\frac{16}{3}\right) \cdot \frac{G'_{deff\_f} \cdot B_f \cdot d_{cri\_f}}{P_{Tf} \cdot L_f} = 0.49$$

$$C_c := \left(\frac{16}{3}\right) \cdot \frac{G'_{deff\_c} \cdot B_c \cdot d_{cri\_c}}{P_{Tc} \cdot L_c} = 1.17$$

Code factors

$$Z := 0.36 \qquad R := 1 \qquad N(T, D) := 1$$

$$C_{h\_f} := 1.65 \qquad C_{h\_c} := 2.29$$

Actual site hazard coefficient NZS 1170.5 Eq 3.1(1)

$$C_{act\_f} := Z \cdot R \cdot N(D, T) \cdot C_{h\_f} = 0.59$$

$$C_{act\_c} := Z \cdot R \cdot N(D, T) \cdot C_{h\_c} = 0.824$$

%NBS for diaphragms

$$P_{NBS\_f} := \frac{C_f}{C_{act\_f}} = 82\% \qquad P_{NBS\_c} := \frac{C_c}{C_{act\_c}} = 142\%$$

Forecast diaphragm displacement at design loading

$$d_{for\_f} := \left(\frac{3}{16}\right) \cdot \frac{C_{act\_f} \cdot P_{Tf} \cdot L_f}{B_f \cdot G'_{deff\_f}} = 122\ mm$$

$$d_{for\_c} := \left(\frac{3}{16}\right) \cdot \frac{C_{act\_c} \cdot P_{Tc} \cdot L_c}{B_c \cdot G'_{deff\_c}} = 63\ mm$$